

Mechanics Model of Plug Welding

Q. K. Zuo¹

University of Alabama in Huntsville, Huntsville, AL, 35899

A. C. Nunes, Jr.²

NASA Marshall Space Flight Center, MSFC, AL, 35812

An analytical model has been developed for the mechanics of friction plug welding. The model accounts for coupling of plastic deformation (material flow) and thermal response (plastic heating). The model predictions of the torque, energy, and pull force on the plug were compared to the data of a recent experiment, and the agreements between predictions and data are encouraging.

Nomenclature

ω	= spinning rate of the plug
R	= radius of the hole in workpiece
δ	= layer thickness of workpiece metal stuck on plug
ϕ	= taper angle of the plug
V_p	= plug pull velocity
q	= heat flux due to plastic heating
T	= temperature
K	= thermal conductivity
$L(t)$	= radius of heat diffusion
τ	= shear strength
P	= pressure

I. Introduction

Plug welding is a process used to close holes left in welds by the Self-Reacting Friction Stir Welding (SR-FSW) process. In the standard Friction Stir Welding (FSW) process a rotating threaded pin is inserted into a weld seam and translated down the seam to stir the sides of the seam together. A shoulder attached to the tool above the pin prevents the weld metal from emerging out of the pressurized zone around the pin, which, if allowed, would leave a furrow, not a weld behind the tool. The pin and shoulder is pressed against the workpiece with a large force (typically tons). An “anvil” supporting the workpiece from beneath provides a reaction force to balance the tool force.

The SR-FSW process was invented for the purpose of avoiding the need for heavy anvil support, which may be difficult to provide where space is limited and is always expensive. In the SR-FSW process a shoulder is attached to the pin bottom, and the pin is pulled up through a hole in the workpiece against a second shoulder. The two shoulders, which rotate with the pin, exert a “squeeze force” on the workpiece that prevents escape of metal from the weld in SR-FSW just as the “plunge force” does with the standard FSW tool.

As the standard FSW pin is withdrawn from the weld, the weld metal flows in beneath it resulting in a completed weld. The SR-FSW pin can be removed from the workpiece only by stopping the weld and either detaching the pin bottom shoulder or detaching the pin from the upper shoulder so that the pin may be extracted from the weld. This leaves a hole in the weld. The hole is customarily filled in by a plug weld. A sketch of the plug weld process is shown in Fig. 1.

A great deal of progress has been made in understanding the FSW process. Less has been made in understanding the plug welding process. The FSW process, as complex as it is, is essentially a steady-state process. As will be seen later in this report, the plug welding process is a transient process with more parameters to be accounted for and is

¹ Associate Professor, Dept. of Mechanical and Aerospace Eng. zuo@eng.uah.edu, AIAA Associate Fellow.

² Analyst, Materials and Processes Laboratory, Engineering Directorate.

therefore inherently a more difficult study. The object of this research is to develop a mechanics model of the plug welding process which, once validated, can be used to improve designing of plugs and selection of weld parameters for different plate thicknesses, hole diameters, and materials.

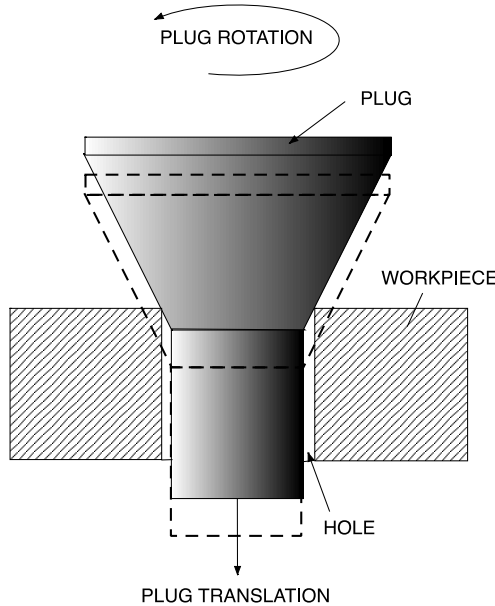


Figure 1. Sketch of plug weld process (a much-simplified plug is shown). Plug is rotated and pulled into hole in workpiece. Workpiece contact metal is extruded out along the contact surface.

II. Mathematical Model

A. Temperatures

Consider the interaction between the plug and the workpiece. Let the plug surface be represented by a plug bonded to the workpiece metal, as shown in Fig. 2. The plug moves into the paper with velocity approximately ωR , where ω is the spinning rate of the plug and R is the radius of the hole in workpiece, and the workpiece is stationary; the plug sticks at the plug/workpiece surface and a thin layer of workpiece metal, of thickness δ , which may vary along the plug surface. (In this study δ is treated as constant along the plug surface).

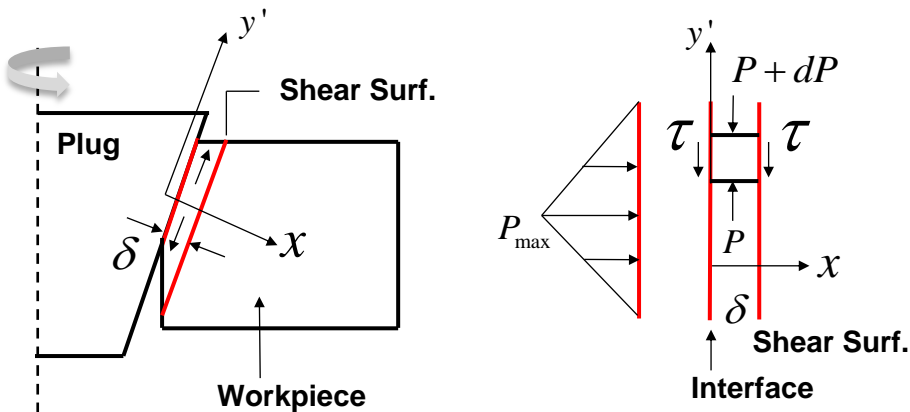


Figure 2. Simplified interface model of the plug and workpiece interaction.

If the shear stress of the weld metal at the interface temperature is τ , then the interface represents a heat source (flux) of magnitude $q = \tau \omega R$. For a constant pull velocity V_p , the depth of penetration (along the thickness of the

workpiece) is $V_p t$, as shown in Fig. 3. Consider unit length along the circumferential direction. The area of the plug-metal interface is then $V_p t / \cos(\phi/2)$, where ϕ is the taper angle of the plug. The rate at which the heat is generated by the heat flux q over the contact area is then

$$\dot{Q}_g = (1) \frac{V_p t}{\cos(\phi/2)} q \quad (1)$$

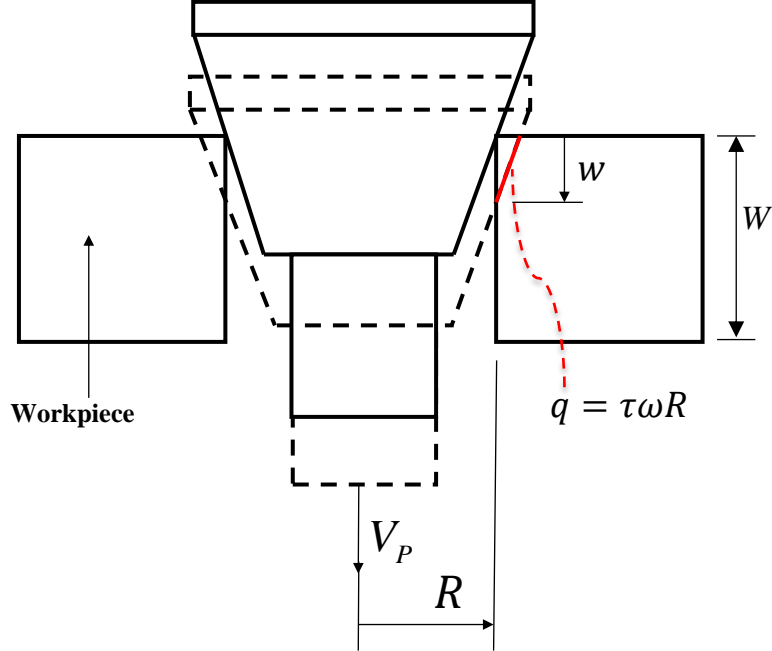


Figure 3. Plug and workpiece interaction showing contact surface and heat flux.

The heat generated is diffused into the workpiece. Let the interface temperature be T and the ambient temperature of workpiece be T_∞ . It is assumed in this work that the heat will be diffused radially into the workpiece. The radius of heat diffusion is taken to be¹

$$L(t) = 2 \sqrt{\frac{\bar{K}}{\rho c} t} \quad (2)$$

where \bar{K} is the “effective” thermal conductivity and is related to the thermal conductivity of the material K by a factor f : $\bar{K} = fK$; ρ and c are, respectively, the density and specific heat of the material. The factor f is introduced such that the heat loss to the materials beyond the radius of heat diffusion $L(t)$ is insignificant. Our analysis of a heat source suddenly applied at a point in infinite solids indicates that a value of $f = 1.5$ gives the radius of heat diffusion that contains more than 90% of the applied heat. Consequently, \bar{K} is taken as $1.5K$.

For a given time t the materials beyond the radius $L(t)$ are regarded as unaffected by the plastic heating. Consider unit length of workpiece (perpendicular to plane shown in Fig. 3). The volume of the material that has been affected by heating is approximated as

$$V(t) = (1) \frac{\pi}{4} L^2(t) = \pi \frac{\bar{K}}{\rho c} t \quad (3)$$

The temperature of the workpiece metal inside the heat diffusion radius is taken as the interface temperature and that beyond the radius of diffusion remains at the ambient temperature. The rate of heat absorption by the workpiece is then

$$\dot{Q}_{abs} = \rho c \dot{V}(t)(T - T_{\infty}) = \pi \bar{K} (T - T_{\infty}) \quad (4)$$

It follows from consideration of energy conservation that

$$\frac{\omega R V_p}{\cos(\phi/2)} \tau t = \pi \bar{K} (T - T_{\infty}) \quad (5)$$

It follows from Eq. (5) that $T < T_m$ for finite values of ω , V_p , and time t , in agreement with physics. In the equation the flow stress at the interface τ depends on the interface temperature T ; hence a model of the flow stress as a function of the temperature needs to be prescribed.

B. Strength Model

Based on the available data on the strength of the workpiece material (2219 aluminum) as a function of the temperature,² a simple, piecewise linear, model $\tau = \tau(T)$ has been constructed (the detail description of the model is reported in Ref. 3). A comparison the model results with the data is shown in Fig. 4. It is seen that the model gives a very good representation of the data.

Substitution of the strength model $\tau = \tau(T)$ into Eq. (5) yields a nonlinear algebraic equation for the interface temperature T as a function of the penetration time t , which is solved by an iterative algorithm (e.g., Newton's method). The resulting temperature $T(t)$ is then used to calculate the strength of the metal at the interface, $\tau(t)$.

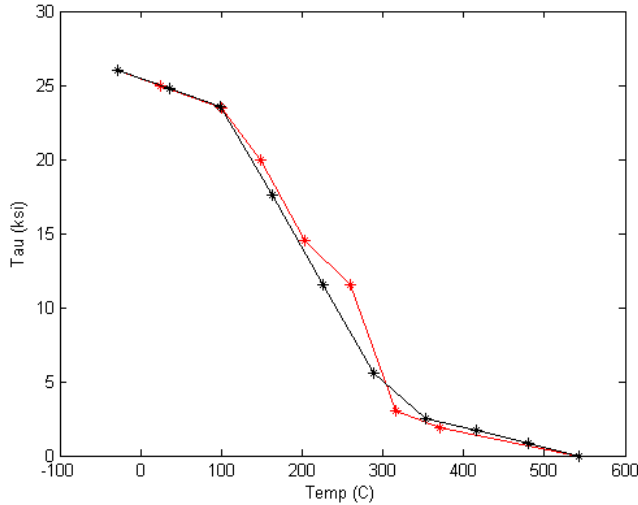


Figure 4. Comparison of the strength given by the piecewise model (black line) and the data (red stars). The model gives a very reasonable representation of the data.

C. Pressure Distribution

Consider the plastic deformation of workpiece metal between interface and the shear surface. It is seen from the micrograph of plug/workpiece contact surface, as shown in Fig. 5, that the metal between the plug-workpiece interface and the shear surface (inside the workpiece) flows along the interface. We refer to this flow as “channel” flow. The cause of this flow is the pressure gradient in the direction of the interface.

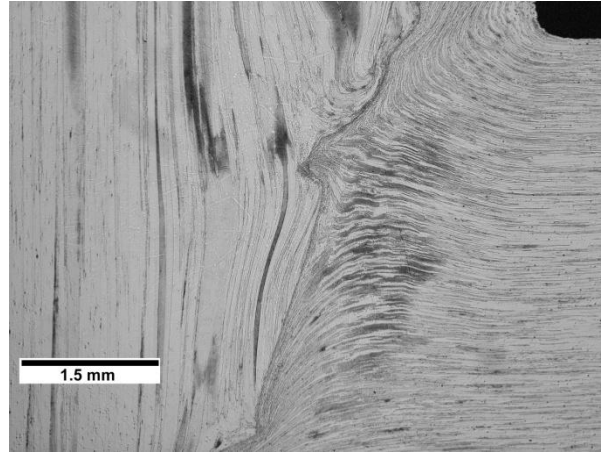


Figure 5. Micrograph (Courtesy of J.C. McClure) showing plug/workpiece contact surface. Flat elongated grains of the rolled workpiece on the left mark a workpiece-side flow against the plug surface, straight in at the center, upswept above and down swept below, as the plug forces the workpiece metal out of its way. Very close to the plug interface the workpiece grain structure vanishes and is replaced by a refined structure; this is thought to be due to passage through a shear surface (adiabatic shear band) separating metal rotating with the plug from the stationary metal of the workpiece.

As the plug is pulled through the hole of the workpiece, the length of the hole that has been pushed by the plug expands radially under the pressure on the interface (to make room for the plug, which deforms much less than the workpiece and hence has been modeled as rigid in this work). To conserve the volume the workpiece metal in the channel must flow (or “squeezed out”) laterally (along the interface) as it expands radially. In order for the metal to flow laterally, the pressure gradient (along the interface) must be large enough to overcome the resistance of the metal to shearing (the shear strength).

Consider the distribution of the pressure along the direction of the channel. The pressure reaches maximum in the middle of the contact length and falls off to zero at the edges of the length. The contact length is $w' = w/\cos(\theta/2)$, where $w = V_p t$ is the depth of penetration defined previously. In order for the material to flow along the channel, the pressure gradient must be enough to overcome the shear resistance of the metal. Let the y' axis be along the interface with the origin at the middle of the contact length, as shown in Fig. 2. Then the equilibrium condition for the metal inside the channel is

$$\frac{\partial P}{\partial y'} \pm 2 \frac{\tau}{\delta} = 0 \quad (6)$$

where the plus and minus signs apply to, respectively, the upper flow ($y' > 0$) and the lower flow ($y' < 0$). In the equation τ is the average shear strength of the metal in the channel. Since the thickness of the channel is very small (on the order of $100 \mu\text{m}$), the temperature and the shear strength of the metal do not change significantly across the channel and are taken as constant in the current work. The pressure reduces to zero at the edges of the contact:

$$P(y') = \pm w'/2 \quad (7)$$

The pressure distribution is

$$P(y') = \begin{cases} P_m \left(1 - \frac{2y'}{w'} \right), & 0 \leq y' \leq \frac{w'}{2} \\ P_m \left(1 + \frac{2y'}{w'} \right), & -\frac{w'}{2} \leq y' \leq 0 \end{cases} \quad (8)$$

where $P_m = (w'/\delta)\tau$ is the maximum pressure at the center of the contact surface. a sketch of the pressure distribution along the channel is shown in Fig. 2. In this study the thickness of the channel is chosen to be $\delta = 100\mu m$, which is consistent with the micrograph of plug weld shown in Fig. 5.

With the shear strength and the pressure on the interface solved, the torque, power, and energy applied to the plug can be calculated in straightforward manner (the details are reported in ref. [3]).

III. Comparison with Experimental Data

As an experimental validation the analytic model presented above was applied to the plug welding experiment.⁴ The experiment was run under the following conditions: $V_p = 27\text{ IPM}$, $\omega = 6,300\text{ RPM}$, $\phi = 13^\circ$, $R = 0.6875\text{ in}$, $W = 0.625\text{ in}$. In addition to the parameters specified by the experiment conditions and the strength model, the following thermal properties for aluminum 2219 were used in the calculations: $\rho = 2,830\text{ kg/m}^3$, $c = 860\text{ J/(kg}\cdot\text{K)}$, $K = 170\text{ W/(m}\cdot\text{K)}$, and $T_m = 543\text{ }^\circ\text{C}$.

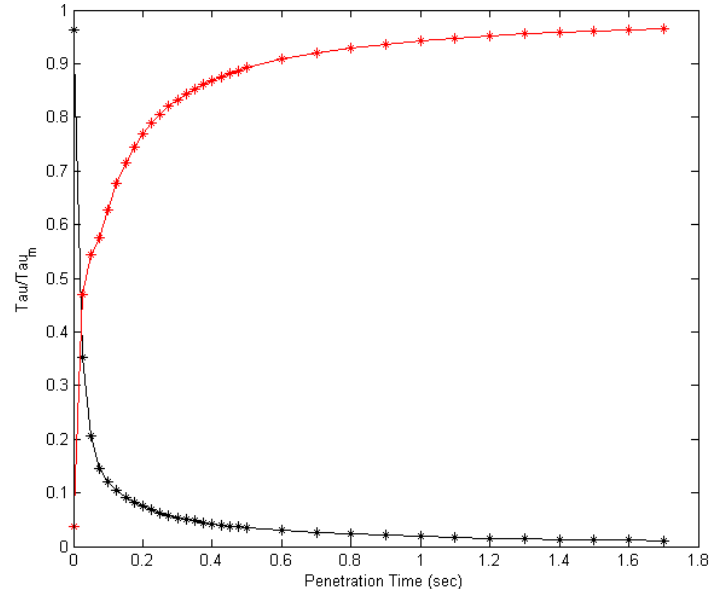


Figure 6. The normalized interface temperature (red) and material strength (black) as functions of penetration time. The temperature and strength are normalized by, respectively, the melting point ($T_m = 543\text{ }^\circ\text{C}$) and the strength of cold metal (τ_c).

The results of interface temperature T and the material strength τ , using the parameters given above, are shown in Fig. 6. It is seen that the interface, starting at the ambient temperature and very high shear strength ($\tau \approx \tau_c = 26\text{ ksi}$), is heated up rapidly by the intense heating flux ($q = \tau\omega R$) initially. As the interface gets hotter, the shear strength reduces, leading to smaller heating flux, and hence slower increasing in the interface temperature, as expected from physics. Figure 6 clearly show the transit nature of the plug-weld process, which is accounted for in the current model.

The model predictions of the torque, energy input, and pull (plunge) force as functions of the penetration time are compared with the experimental data,⁴ as shown in Figs. 7-8. Note the time here is measured from when the penetration first occurs (i.e., plug starts to engage the work-piece metal). It is seen that the model gives reasonable predictions of the torque, energy input, and the pull force.

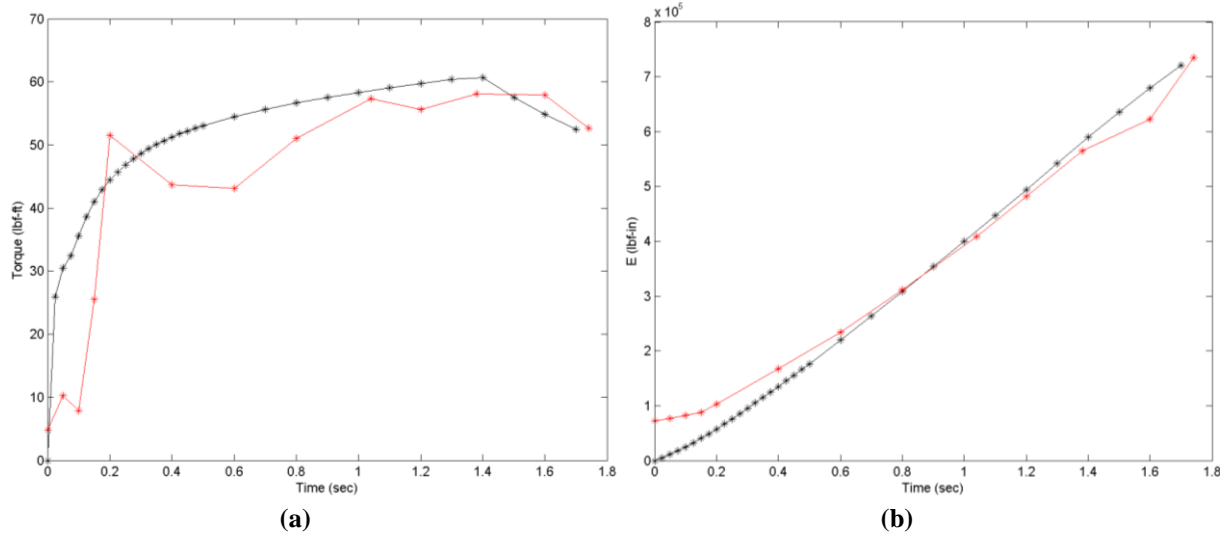


Figure 7. Comparison with the data of the predicted torque (a) and energy (b). The data is shown as red.

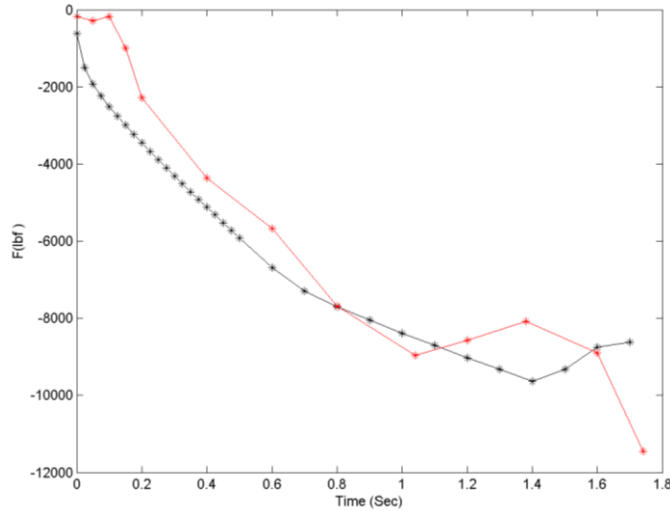


Figure 8. Comparison of the predicted history of pull (plunge) force and the data. The data is shown as red.

IV. Conclusion

The following are some observations and preliminary conclusions resulted from this study:

1. In plug welding processes the transient nature of heat transfer needs to be accounted for, whereas Friction Welding Process can be treated, to good accuracy, as steady-state.

2. For the plug weld experiment⁴ the model predicts that the interface will reaches a temperature of $0.97T_m$ at 1.5 seconds of the travel time (penetration of the plug). This is consistent with the experiment, where local melting is believed to have occurred in the neighborhood of the bond-line (plug/workpiece interface).

3. Furthermore, comparisons of the predicted torque, energy and pull force with the data are rather encouraging.

It should be pointed out however that much still needs to be done on the model before we can consider it a truly useful model for plug welding. Specifically, the assumption of radial diffusion of heat (from the contact surface) seems to be physically plausible, but is nevertheless an assumption, the validity of which should be more carefully examined. Furthermore, for simplicity, the model has not considered the deformation (plastic flow) of the plug nor has it explicitly considered local partial melting of the materials, which has been observed in the experiments. We plan to pursue these issues in the future.

Acknowledgments

We are grateful to Po-Shou Chen and Justin Littell for the experimental data of plug welding and for explaining various features observed in the experiments. We also thank Judy Schneider and Carolyn Russell for technical discussions and organizational support.

References

- ¹Crank, J., *The Mathematics of Diffusion*, Oxford University Press, 1975, Chap. 1.
- ²Davis, J.R., et al., *Metals Handbook* (10th Edition), Vol 2 (Properties and Selections: Nonferrous Alloys and Special-Purpose Materials, ASM International, 1990, pp. 79-81.
- ³Zuo, Q.K., “Mechanics Model of Plug Welding”, *Report to NASA Marshall Space Flight Center (EM 32)*, August, 2015 (unpublished).
- ⁴Cleghorn, D., Hepburn, F., Girgis, A., Chen, P. and Littell, J., “SLS 0.625” Friction Pull Plug Weld Development”, *NASA Technical Report* (to be published).